J. Synchrotron Rad. (1998). **5**, 437–439

The operation of a superconducting wiggler at TERAS

S. Sugiyama,[a]* H. Ohgaki,[a] K. Yamada,[a] T. Mikado,[a] M. Koike,[a] T. Yamazaki,[a] S. Isojima,[b] C. Suzawa[b] and T. Keishi[b]

[a]Electrotechnical Laboratory, 1-1-4 Umezono, Tsukuba City, Ibaraki 305, Japan, and [b]Sumitomo Electric Industries Ltd, 1-1-3, Shimaya, Konohana-ku,Osaka 554, Japan. E-mail: ssugiya@etl.go.jp

(*Received 4 August 1997; accepted 28 November 1997*)

A superconducting wiggler has been successfully installed at the ETL 800 MeV electron storage ring facility (TERAS). The operation of the wiggler at magnetic field strengths of 5 T with electron beam energy of 750 MeV has been accomplished. The wiggler has been designed and constructed to produce synchrotron radiation with critical photon energy around 3 keV for scientific, industrial and medical applications. We report here experiments that demonstrate the possibility of stable operation of a superconducting wiggler in a small storage ring.

Keywords: superconducting wigglers; magnet training, magnetic field analysis; betatron tune shift.

1. Introduction

Because of the increasing demand for non-invasive methods in coronary angiography using synchrotron radiation, a small synchrotron radiation source at reduced cost is desirable (Dix, 1995). Such dedicated storage rings need to produce hard X-rays at 33 keV in sufficient intensity. The superconducting wiggler project at TERAS was started in order to study the operation of a high magetic field wiggler at a small storage ring (Sugiyama *et al.*, 1992), as the insertion of superconducting wigglers at small storage rings could generate the hard X-rays necessary for coronary angiography.

Because the superconducting wiggler produces nonlinear magnetic field components in the storage ring, intensity losses from the stored electron beam can result. Another difficulty encountered in the design and construction of the wiggler was the distortion of the superconducting coil by strong electromagnetic forces. In this report we describe the construction of the wiggler magnet and the influence of the wiggler on the storage ring based on magnetic field analysis using a three-dimensional finite-element method.

2. The structure of the wiggler

The wiggler magnet, a hybrid of Nb_3Sn and NbTi, consists of three pairs of superconducting coils with iron poles. The two outer pairs are used to correct the beam orbit. In order to generate a sufficiently strong magnetic field, the bore of the wiggler is kept at cryogenic temperatures by a helium cryostat, described below. The magnet gap was chosen to be 28 mm. It was inserted in a straight section of length 1.8 m between two correcting quadrupole magnets. The total length of the wiggler magnet is 700 mm. Its central (racetrack) coils consist of three sections: the inner 1.25 mm diameter Nb_3Sn windings are separated from the outer 1.4 × 0.7 mm NbTi wound coils by support collars, which protect the coils from distortion by electromagnetic forces.

Magnet training by repeated quenching started at 5.8 T and reached a maximum of 7.63 T (172 A) as shown in Fig. 1. A one-off malfunction caused the stored energy at 7.63 T to be dumped in the magnet and the protection resistor. (The main magnet coil is designed with a quench protection resistor across the terminals of the power supply.) This could account in part for the subsequent degradation of the peak achievable current. After the malfunction, quenches occurred at slightly lower currents. It is thought that this is owing to the brittle nature of the Nb_3Sn wire. At the end of training, the central coil could produce a maximum field strength of 7.4 T with an exciting current of 167 A.

The limits on the magnetic performance of the wiggler depend on the quench energy of the Nb_3Sn wire and the maximum sustainable strain on the superconducting coils, which are impregnated with epoxy resin and mechanical compression frames. If the stress distribution induced by the electromagnetic forces produces significant strain, micron-scale movement takes place and results in a release of strain energy in excess of the quench energy. A theoretical estimate of the value of the strain energy at quench fields gave a value of 1.35 mJ at 9.1 T. However, such high quench fields were not achieved on the real wiggler, in part because of the difficulty in controlling local stresses in an epoxy resin system.

The magnetic field is monitored using Hall sensors specially designed for low-temperature operation and calibrated beforehand. The Hall sensors, 6 mm in diameter and 3 mm thick, were embedded and glued with epoxy resin in the hollows of the magnet on the surface of the soft iron poles.

The 1.8 m-long straight section was not long enough to install the wiggler and the quadrupole magnets used for local correction in the short drift space between the wiggler and the dipole bending magnets. Therefore, smaller focus-correction quadrupole magnets were installed, resulting in further beam intensity losses as described in the next section.

The cryostat used to keep the wiggler at cryogenic temperatures consisted of a conventional helium bath surrounded by a liquid-nitrogen-filled jacket to intercept radiated heat. The metallic radiation screens were also in thermal contact with the liquid-nitrogen jacket. The vacuum space between the liquid-nitrogen container and the outer shell was filled with many layers of superinsulation. This configuration required 8.5 l of liquid

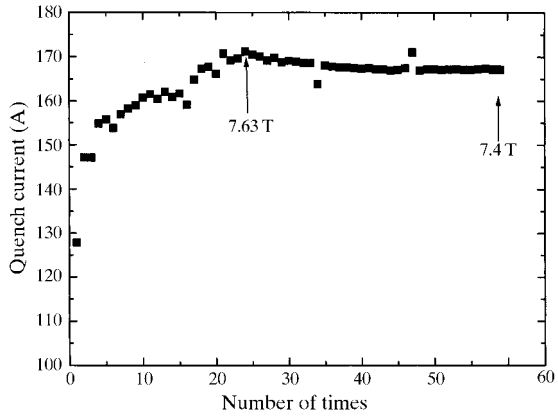

Figure 1
Training of the wiggler magnet in the three-pole operation mode.

helium per hour during operation. In order to minimize liquid-helium consumption during the initial cooling, the transfer was carried out over five hours and required 220 l of liquid helium. Work to improve the helium consumption of the wiggler is in progress, by using a high-temperature superconducting material for the current leads and a small helium-exchange gas refrigerator for the cryostat.

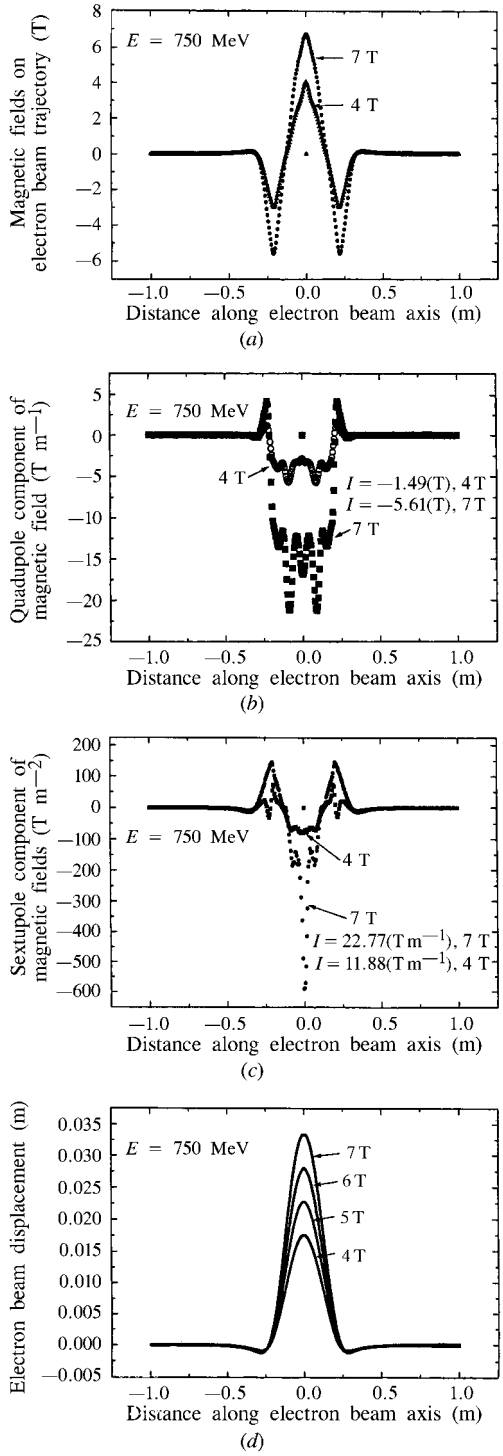

Figure 2
The dipole (*a*), quadrupole (*b*) and sextupole (*c*) components of the magnetic field for beam orbits in different operating conditions; (*d*) electron-beam trajectories.

3. Magnetic field analysis

Computer-simulated magnetic field analysis was achieved using a three-dimensional static field computation. Three-dimensional finite-element analyses were carried out using *JMAG* (Ikeda, 1990), which uses the two-vector potential method to simulate the wiggler and its iron core.

The largest contribution to the field is, of course, from the coils, as the iron parts of the magnets are highly saturated. The exciting currents of the three coils were adjusted so that the first and second integration of dipole field strengths B_y along the electron-beam trajectory were 2.03×10^{-4} and 2.05×10^{-4} Tm, respectively, for operation at 5 T. The distribution of field strengths gives a dipole component B_y on the beam trajectory in the mid plane of the wiggler as shown in Fig. 2(*a*). Quadrupole and sextupole components along the same trajectory are shown in Figs. 2(*b*) and 2(*c*), respectively. It can be seen that the wiggler generates a large change in the quadrupole component along the beam trajectory in the region where the electron beam makes a large excursion at 7 T operation. The profiles in Fig. 2(*d*) repre-

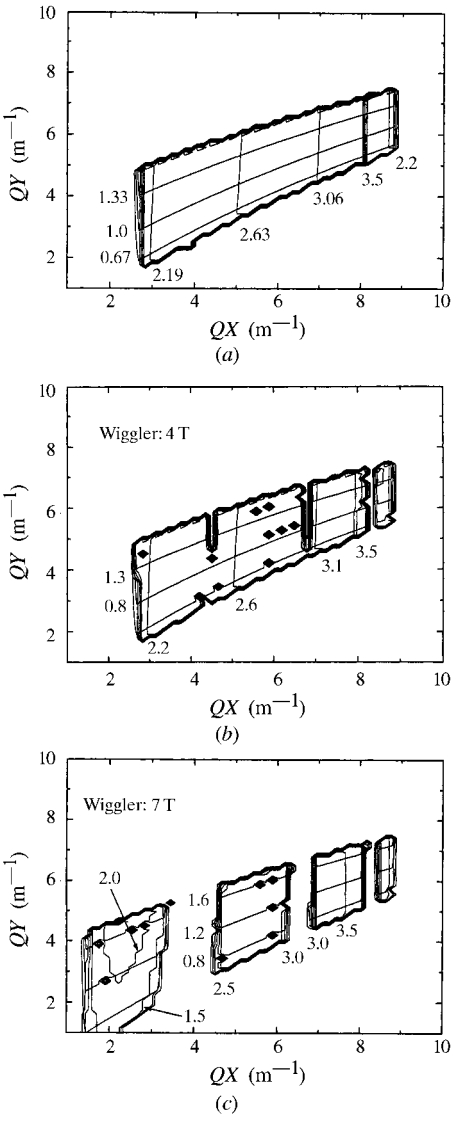

Figure 3
The tune regions for a stable beam for various operating conditions of the wiggler: (*a*) non-operation, (*b*) operation at 4 T and (*c*) operation at 7 T.

sent beam trajectories under different field strengths at a fixed electron energy of 75 MeV. A fourth-order Runge–Kutta method was used to compute the electron trajectories.

Fig. 3 shows some of the betatron tune diagrams of the storage ring under different operation fields of the wiggler. In the tune-diagram simulation, the wiggler is modelled as a magnet sliced in the horizontal central plane into very small elements of length *ds* (5 mm) along the beam trajectory. The dipole and quadrupole components of the magnetic field within each wiggler element were assumed to be uniform. The transfer matrix of each element was calculated for radial and vertical matrix elements according to the electron equation of motion (Brown, 1968). Compensation-magnet components were not included in the simulation. Fig. 3 shows that the operation of the wiggler produces gaps in the stability region along some resonance lines. This confirms the violent nonlinear effects on the lattice observed at high magnetic field operation. These effects result in a degradation of the electron beam quality and add to the difficulty of operating the wiggler.

4. Wiggler operation

Wiggler operation was carried out up to 5 T with electron-beam energy of 750 MeV by continuously correcting the tune shift with the main defocusing quadrupole magnets and the small focusing correction quadrupole magnets near the wiggler. Fig. 4 shows plots of the exciting currents of the main defocusing quadrupole magnets and the focusing correction quadrupole magnets as a function of the magnetic field. Because the injection electron beam can oscillate with a large amplitude in the wiggler, the wiggler was not powered up until the beam accumulation in TERAS and the electron energy had been ramped up to 750 MeV. Above 5 T a spread in the vertical betatron tune occurred and it was difficult to make any adjustment. At higher magnetic fields, there was considerable electron beam loss and the operation had to be aborted.

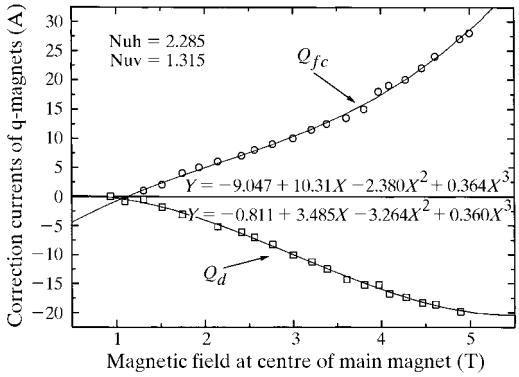

Figure 4
Plots of the exciting currents of the main defocusing quadrupole magnets and the correcting focusing quadrupole magnets as a function of magnetic field. Nuh: horizontal betatron tune; Nuv: vertical betatron tune.

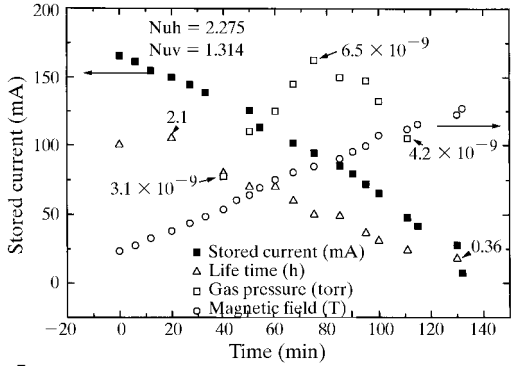

Figure 5
Decay plots for the stored electron beam and life time as a function of the ramping time of the exciting current at 750 MeV. Nuh: horizontal betatron tune; Nuv: vertical betatron tune.

According to theory, in an ideal plane wiggler the vertical tune shift scales as the square of the wiggler field strength (Pool & Walker, 1985). As a result of the horizontal component of the electron velocity, there are also edge defocusing forces and changes in vertical deflection which cause a shift in the vertical betatron tune. For the wiggler, there is a large horizontal excursion in the trajectory of lower energy electrons. The tune shift has a linear dependence on this horizontal displacement (Kulipanov, 1990). The curves of focusing and defocusing correction-magnet currents shown in Fig. 4 are described well by second-order polynomial functions of the wiggler exciting current. This is consistent with the premise that the betatron tune shift results from two different effects: one is second order, corresponding to the magnetic field of the wiggler, and the other is first order, arising from the large horizontal excursion of the electron beam trajectory.

Another effect that decreased the electron-beam life was a degradation of the vacuum in the ring. As the field strength of the wiggler was raised, the pressure in the ring increased because of gas desorption from the vacuum chamber induced by high-energy synchrotron radiation. Fig. 5 shows decay plots of the stored electron beam and life time as a function of the ramping time of the exciting current. The ramping speed of the exciting current was 3 A min^{-1} (corresponding to 0.125 T min^{-1}). The shift of the betatron tune was almost constant because the field strength was ramped slowly and the quadrupole magnets were continually adjusted. The beam stability was not improved by increased r.f. power under operation at fields higher than 5 T.

5. Conclusions

A superconducting wiggler was operated up to 5 T in a 750 MeV electron beam at TERAS. The magnetic field of the wiggler was analysed using a three-dimensional finite-element method and electron-beam characteristics were simulated under different operation fields of the wiggler. The experimental results indicate that at higher field operation, the stored electron beam is affected considerably by the nonlinear component of the magnetic field of the wiggler.

References

Brown, K. L. (1968) *Advances in Particle Physics*, Vol. 1, edited by R. L. Cool & R. E. Marshak, pp. 71–134. New York: Interscience.
Dix, W. R. (1995). *Prog. Biophys. Mol. Biol.* **63**, 150–192.
Ikeda, F. (1990). *JMAG.* The Japan Research Institute Limited, 16 Ichiban-chou, Chiyoda-ku, Tokyo, Japan.
Kulipanov, G. (1990). *Insertion Devices. First ICFA School on Beam Dynamics & Engineering of Synchrotron Light Sources.* International Atomic Energy Agency, United Nations Educational, Scientific and Cultural Organization, International Center for Theoretical Physics, ICTP, PO Box 586, 341000 Trieste, Italy.
Pool, M. W. & Walker, R. P. (1985). *IEEE Trans. Nucl. Sci.* **32**, 3374–3376.
Sugiyama, S., Ohagaki, H., Mikado, T., Noguchi, T., Yamada, K., Chiwaki, M., Suzuki, R., Koike, M., Yamazaki, T., Tomimasu, T., Keishi, K., Usami, H. & Hosoda, Y. (1992). *Rev. Sci. Instrum.* **63**, 313–316.